



27th October 2021

Available online at <https://conference.rsujnet.org/>

Paper number: ICNET2021-013

Development and Performance Evaluation of an Improved Garri Mash Sifter

Nnanna C. Ajanwachuku¹, Silas O Nkakini², Asinyetogha H. Igoni²

¹Department of Postharvest Engineering Research

Nigerian Stored Product Research Institute, Port Harcourt Zonal Office, Nigeria.

²Department of Agricultural and Environmental Engineering, Faculty of Engineering

Rivers State University, Nkpolu-Oroworukwo, Port Harcourt, Nigeria

ahigoni@yahoo.com; +234(0)802-312-3471

ABSTRACT

Sifting of dewatered cassava mash lump into finer particles to remove oversized grain fractions is a key process in the cassava-to-garri production chain. However, to eliminate the problems associated with the traditional method of garri sifting in Nigeria, a motorized garri sifting machine was designed, fabricated, and tested. The machine design employed the fundamental principle of vibratory motion associated with rotor dynamic systems. It consists of the mainframe, hopper, sifting chamber, pulley, belt arrangement and the discharge outlet; and powered by two electric motors of 1-horsepower (0.745 kW) rating with angular speed of 1,725 rpm. The sifting action is achieved by an induced vibratory motion, generated by the rotation of the camshaft in the pulley and belt arrangement. The results of the performance evaluation of the machine showed a throughput capacity of 124 kg/hr, while the sifting capacity was 164 kg/hr, with an average sifting rate of 0.047 kg/s, resulting in an overall sifting efficiency of approximately 76%. The development of this machine has improved the timeliness of the garri sifting process and eliminated the drudgery and hazards associated with the prevalent manual sifting process.

KEYWORDS: cassava mash, continuous flow, garri, sifting machine, vibratory motion, performance evaluation, drudgery.

Cite This Paper: Ajanwachuku, N. C., Nkakini, S. O., & Igoni, A. H. (2021). Development and Performance Evaluation of an Improved Garri Mash Sifter. *Proceedings of the International Conference on Newviews in Engineering and Technology Maiden Edition*, Faculty of Engineering, Rivers State University, Port Harcourt. Nigeria, 27th October 2021, ICNET2021-013, 148 – 159.

1.0 INTRODUCTION

Cassava (*Manihot esculenta* Crantz) is a major source of carbohydrate in most developing nations of the world. In our country Nigeria, cassava crop can be processed into garri, lafun, pellets and chops for direct paki “pupuru”, “fufu”, cassava pellets and chips for the direct human and livestock consumption (Alonge *et al.*, 2012). In many countries of Sub-Saharan Africa, it is the cheapest source of calories available. In addition, the roots contain significant amounts of vitamin C, thiamine, riboflavin, and niacin (FAO, 1997). These sterling qualities that cassava possesses make it imperative to note that a number of countries, including Nigeria, have identified the need for the adoption of cassava as a major staple food thus encouraging its production. Amongst cassava products such as fufu, garri, amala, starch, abacha, cassava chips and flour, garri is the most popular. Garri being considered as the most preferred form in which cassava is utilized, a lot of concern has been placed on its processing, preservation, and storage. The conversion of whole cassava tubers into staple foods like garri involves a number of processing operations. Each of these processing operations contributes a certain factor to the stability of garri when it is eventually turned into the gelatinized form. Sifting of garri turns out to play a key role in producing an end-product of better and more uniform quality and reduces the drudgery and intensive labour associated with sieving manually.



27th October 2021

Available online at <https://conference.rsujnet.org/>

A lot of research works have been conducted in the area of garri processing and most attention directed towards small and medium scale processing.

Sulaiman and Adigun (2008) fabricated a cassava lump breaker but failed to conduct a comprehensive performance evaluation in terms of the efficiency and throughput capacity on the machine. Alabi (2009) developed a motorized cassava lump breaker and sifting machine but recommended that an outlet provision should be made for unsifted materials, cover for the hopper, and a cover should be made for the pulley and electric motor for the protection of the operator. Kudabo *et al.* (2012) developed and evaluated a motorized cassava mash sifter, which was powered by an electric motor. Jackson and Oladipo (2013) developed and evaluated a motorized dewatered cassava mash sifter to determine the effects of operating speed on its sifting efficiency. According to Ahiakwo *et al.* (2015), all designs mentioned were silent with respect to the sieve aperture sizes that were used to produce the speeds, outputs, and efficiencies. Hence, Ahiakwo *et al.* (2015) appraised available sieving technology and made projection for developing an effective sieving technology. Ovat and Odey (2018) developed, fabricated, and evaluated a motorized garri sieving machine incorporating new features such as a lump breaking

pot, aluminum sieving chamber to prevent corrosion and rusting, guards on running parts to ensure the safety of the operator and improve machine life and the use of links in place of cams and followers. Although comprehensive, Ovat and Odey's design and the others were of a batch flow nature which invariably affects large scale production. Although the rotary type dewatered

cassava mash sifter developed by Igoni (1991) was of a continuous flow nature, the efficiency produced was 56% due to the type of sieve used. Therefore, there is need to develop an improved continuous flow type dewatered cassava mash sifter using a reciprocating sieve which is designed for high capacity and efficiency of operation. Hence, this study is aimed at improving the efficiency of an existing design of a continuous flow type rotary sieving machine for garri processing.

1.1 The Flow Diagram of Garri Production

The flow chart indicates the flow of cassava tuber through the various processing units to the last processor to obtain garri. It consists of the fresh cassava tubers, manual peeling of the cassava, and grating of the peeled cassava, pressing the dough, sifting the squeezed dough, frying, and drying of the sifted cassava.

Factors considered for the theoretical development of the machine include those that will minimize power requirement and cost of the machine, and increase sieving efficiency. These factors are enumerated below.

i. **Material specification:** The choice of materials for use in the construction of the sieving machine was based on several intervening factors such as suitability of the material for the desired purpose, availability and cost effectiveness of the material, strength of materials for the fabrication, moisture content of the product to be processed on the machine, corrosion resistance properties, hygiene etc. In these regards, carbon steel, mild steel and galvanized steel plates were used for the fabrication. More so, they would ensure sieve operation hygiene and machine rigidity.

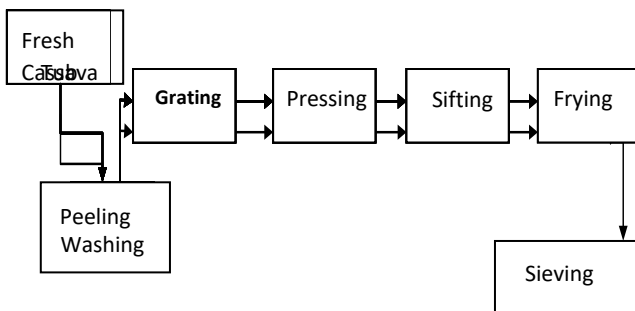


Fig 1: Garri processing flow diagram

2.0 MATERIALS AND METHODS

2.1 Design Considerations



27th October 2021

Available online at <https://conference.rsujnet.org/>

ii. **Type of Sieve:** The type of sieve used is one with an optimum sieve aperture size and specially designed for high capacity and efficiency of operation. In these regards, a vibrating sieve was used for the construction.

iii. **Length of Sieve:** The length of sieve, rate of sieving, forward travel of mash per revolution of sieve, and residence time are all interwoven. According to Igoni (1991), this relationship guaranteed the product coming out at the discharge end should only be chaffs, meaning that sieving would have been completed by the time the products get to the discharge end.

2.2 Design Theory

i) Design of Hopper

The capacity of the sieve hopper was determined using equation 1

$$V_2 = \frac{1}{3} (A_1 + A_2 + \sqrt{A_1 \times A_2}) \times h \quad (1)$$

$$V_2 = 0.010752m^3$$

Where,

V_2 = Volumetric capacity of the hopper.

A_1 = Top area of upper base of hopper ($L \times w$); $L = 0.51 m, w = 0.26 m$

A_2 = Lower base area of hopper ($L \times w$); $L = 0.31 m; w = 0.17 m$

h = Height of the frustum (Hopper) = 0.12 m

Total surface area, (T_{SA}) of hopper = (Area of upper and lower base) + (Area of four trapezoidal faces)

$$T_{SA} = (A_1 + A_2) + \left[\frac{1}{2} (a + b)h \right] \quad (2)$$

$$T_{SA} = 0.0489m^2$$

Where; 'a' and 'b' are the opposite parallel sides of the trapezoid

$$\text{trapezoid} = \frac{1}{2} (a + b)h \quad (3)$$

Area of

ii) Belt Length

For this design, an open belt drive system was adopted because both pulleys rotate in the same direction. Considering the pulley diameters, the length of the belt was determined as:

$$L = \frac{\pi}{2} (d_1 + d_2) + 2x + \frac{(d_1 - d_2)^2}{4x} \quad (4)$$

$$L = 0.8737m (874mm)$$

d_1 and d_2 = Diameters of the larger and smaller pulleys

d_1 and d_2

= 0.108 m and 0.052 m respectively

x = Distance between the centres of two pulleys (310 mm) = 0.31 m

iii) Ratio of Driving Tensions on Belt

For V-belt drive,

$$2.3 \log\left(\frac{T_1}{T_2}\right) = \mu\theta \text{Cosec}\beta \quad (5)$$

Where

T_1 = Tension in belt on the tight side

T_2 = Tension in belt on the slack side

μ = Coefficient of friction between the belt and steel pulley

β = Half the angle of groove on the pulley

iv) Belt Tension

$$T_1 = T - T_c \quad (6)$$

Where

T = Maximum tension in the belt



27th October 2021

Available online at <https://conference.rsujnet.org/>

$T_c =$
Centrifugal tension

Weight of belt per meter length = 1.06 N (Khurmi and Gupta 2005)

$$W = m \times g \quad (7)$$

$$T_c = M \times V^2 = 0.108 \times (4.69)^2 = 2.38 \text{ N}$$

$$T_{max} = \sigma \times a$$

Where $\sigma = 2.5 \text{ Mpa}$ (2.5 N/mm^2)

$a =$ width of belt (b) \times thickness of belt (t)

$$a = 13 \text{ mm} \times 8 \text{ mm} = 104 \text{ mm}^2 \quad (1.04 \times 10^{-4} \text{ m}^2)$$

$$T_{max} = (2.5 \times 104) \text{ N} = 260 \text{ N}$$

$$T_1 = 257.62 \text{ N}$$

$$2.3 \log\left(\frac{T_1}{T_2}\right) = \mu \theta \text{Cosec} \beta$$

$$T_2 = 56.62 \text{ N}$$

v) Power Transmitted by the Belt

$$\text{Power transmitted} = (T_1 - T_2) \times V \quad (8)$$

Where

$T_1 =$ Tension in the tight side of the belt

$T_2 =$ Tension in the loose side of the belt

$V =$ velocity of belt in m/s (4.69 m/s)

vi) Shaft Design

For a solid shaft having little or no axial loading, the ASME code equation from Ndirika and Onwualu (2016) is given as:

$$d^3 = \left(\frac{16}{\pi S_s}\right) \times [(K_b M_b)^2 + (K_t M_t)^2]^{1/2} \quad (9)$$

Where:

$d =$ Diameter of the shaft

$M_t =$

Torsional moment

$M_b =$ Bending moment

$K_b =$ Combined shock and fatigue factor applied to bending moment

$K_t =$ Combined shock and fatigue factor applied to torsional moment.

$S_s =$ Allowable stress

vii) Bending Stress

According to Hall *et al* (2002) bending stress can be determined as follows:

$$S_b = \frac{32 M_b}{\pi d^3} \quad (\text{For a solid shaft}) \quad (1)$$

Where:

$S_b =$ Bending stress (108 N/mm^2)

$M_b =$ Bending moment (38.17 Nm)

$d =$ Shaft diameter (15.33 mm)

viii) Torsional Stress

This can be obtained using the equation below as given by Hassan *et al* (2009).

$$T_{xy} = \frac{16 M_T}{\pi d^3} \quad (\text{For solid shaft}) \quad (11)$$

Where:

$T_{xy} =$ Torsional stress (7.4 N/mm^2)

$M_T =$ Torsional moment ($5.22 \times 10^3 \text{ Nmm}$)

$d =$ diameter of shaft (15.33 mm)

ix) Shear Force and Bending Moments

To convert the torque at the pulley to force, we apply the equation below



27th October 2021

Available online at <https://conference.rsujnet.org/>

$$\text{force} = \frac{\text{Torque}}{(\text{Length of arm} \times \sin\beta)} \quad (12)$$

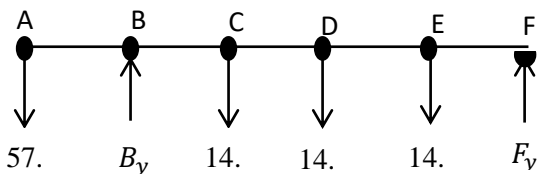
Length of arm,
 L = centre to centre distance between motor pulley and shaft pulley (0.31m)

β = Groove angle (17°)

T = Torque (5.2Nm)

Resolving shear forces and bending moment

a). Reaction calculation and diagram



A = Pulley Node

B = Bearing 1 Node

C = CAM 1 Node

D = CAM 2 Node

E = CAM 3 Node

F = Bearing 2 Node

Calculating moment about A, $F_A = 0$

But summation of all moments about A must be equal to zero i. e. $\sum M_A = 0$

x) **Power Required to Rotate Pulverizing Shaft and Pulley**

The torque and power required to drive the pulverizing shaft and pulley were determined with equations (13) and (14) as presented in Igoni (1991), thus:

$$T_{pp} = \left(W_s \times \frac{d_s}{2} \right) + \left(W_p \times \frac{d_{pp}}{2} \right) \quad (13)$$

$$T_{pp} = 0.9571 Nm$$

$$P = T_{pp} \times \omega_s = 72.74 W \quad (14)$$

xi) **Angle of Repose**

This was obtained using the equation $\tan \phi = \frac{2\pi h}{c}$ (15)

Where

ϕ = angles of repose

h = Height of Mound (cm)

c = Circumference of Mound base

d = diameter of Mound base (Cm)

$$\tan \phi = 0.7442 = 0.8682$$

$$\phi = \tan^{-1}(0.8682)$$

$$\phi = 40.96$$

3.0 RESULTS AND DISCUSSION

3.1 Designed Sieve Dimensions

- i. Hopper dimensions
 - a. Top cross-section = 0.51 x 0.26 m
 - b. Bottom base cross-section = 0.31 x 0.17 m
 - c. Height of frustum = 0.12 m
- ii. Diameters of large and small pulleys, d_1 and d_2 0.108 m and 0.052 m respectively
- iii. Centre distance between the pulleys = 310 mm (0.31 m)
- iv. Weight of belt per meter length = 1.06 N

3.2 Machine Fabrication and Assembly

The materials used for fabricating the machine are: Two (2) inch steel pipe, one (1) and two (2) inch angle bars, 20mm steel shaft, 40mm steel shafts and Steel mesh, bolts, and nut, 3mm steel plate, pillow bearing, roller bearing, 3mm steel rod, and 16mm steel rod. Two (2) inch steel pipe was cut to the predetermined length forming the support structure of the equipment and were linked with four supports of 2-inch angle bar, braced along its length and width forming rigid



27th October 2021

Available online at <https://conference.rsujnet.org/>

structure.

Steel plate was cut and tac weld to one side of the support structure serving as support for the springs and the roller track. A pair of roller track was formed from steel plate and tac weld to the support plate. Furthermore, a rectangular shape was formed with 1-inch angle bar and tac weld to form a rigid structure which function as the frame of the sieve. Evenly spaced holes of 10 mm were drilled along the flange of the angle bar and the sieve was cut to the desired dimension and bolted unto the frame. A steel shaft was cut to the required length and a roller bearing fitted to one end. A tac weld was done in front end behind the bearing in the shaft to prevent longitudinal motion of the bearing. The rollers at the four corners of the rectangular frame were welded. The sieve was mounted unto the roller track, greased, and checked to ensure the motion is unhindered. The point of attachment of the springs was marked, holes drilled and then the springs attached through bolting. A two-inch angle bar was cut to the length of pillow bearing. Holes for pillow bearing were drilled and weld to the support frame as support for drive shaft. Cams were cut and drilled to size of shaft and then arranged on shaft and welded. The bearings were attached to both ends of the shaft and then mounted on the support frame and fastened to the bolt. A pulley was fitted to the drive end of the shaft. Base plate for electric motor was cut and welded to the support frame. Fastening holes were drilled on the plate and then the motor was mounted and fastened to the base plate. The pulleys connection via belt was done and the tensioning bolt welded. The tension bolt was tightened to the desired tension, through which the motor was secured.

The hopper plates were cut to specific dimensions and assembled and welded to from rigid structure. Both shafts in the hopper were cut to the desired length and the end of the driving shaft was machined to the size of the inner diameter of the pulley. Three (3) 3 mm rod was cut into 20 mm length and tac weld to the shaft in an alternating pattern. The shaft was attached to the hopper and

secured in place through end bearing, and the sprockets were attached to the end of both shafts via weld. Driving pulley was attached to the driving shaft. Base plate for electric motor and fastening holes were drilled on the plate. The electric motor was mounted on the base plate and the pulleys were connected via belt. The tension bolt was tightened to the desired tension, through which the motor was secured.

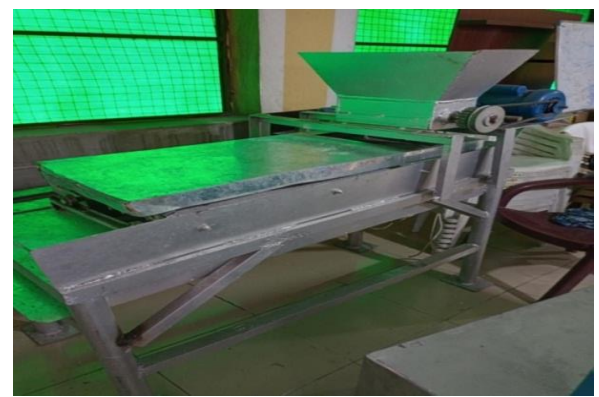


Plate 1: Full view of the fabricated Garri Sieving Machine



Plate 2: Dewatered Garri Mash

27th October 2021

Available online at <https://conference.rsujnet.org/>



Plate 3: Garri Fines (sievate)

3.3 Description of the Sifter

The developed motorized garri sieving machine consists of the following components:

- i. Main frame: the main unit of the machine on which all other components of the machine are supported.
- ii. Hopper: a trapezoidal shaped pyramid through which lumps of dewatered mash cake are fed into the sieving trough through gravity.
- iii. Sieving chamber: a rectangular trough of considerable depth to prevent spilling of agitated particles during operation and length to ensure that the product coming out at the discharge end of the sieve would be chaff alone, that is sieving would have been completed by the time the products get to the discharge end.
- iv. Pulley and Belt: The pulley and belts are preferred to this purpose as the distance between the two pulley is short, resulting in negligible slip between pulleys, easy installation, long life, high velocity ratio, high power transmission and its ability to absorb shock.
- v. Discharge outlet: this consists of the outlet chute for the fines (under-sized particles).
- vi. Electric motor: this provides the power needed to operate or run the machine.

- vii. Bearings: this is used to provide support for the shaft and reduce friction between moving parts which can cause a loss of available power.
- viii. Camshaft: this is used to transmit power from one place to another.

Basically, power generated by the 1-hp electric motor is delivered to the camshaft- a device which converts rotational motion to reciprocating motion. The motion generated because of the rotation of the camshaft in the pulley and belt arrangement is further transmitted to the sieve housing thus providing the forward throw while the spring positioned in the opposite direction returns the sieve on the backward throw. This to and fro linear movement (reciprocating action) of the sieve housing leads to the sifting action of the pulverized garri mash.

3.4 Performance Evaluation of the Machine

The machine was tested using a two 1 hp single phase electric motor at 2 kg, 7 kg, 12 kg, 17 kg and 22 kg loading respectively. Test samples used for the performance evaluation of the machine were processed through the raw cassava to the required product (dewatered cassava mash). The different masses of dewatered cassava mash were weighed on a weighing scale and varied with a constant motor speed of 1725 rpm at different intervals. Each mass of cassava mash beginning with 2 kg was fed into the hopper, which in turn was properly spread out into the sieving chamber. The machine was running until the cassava mash was completely sieved. Important parameter such as the mass of garri sieved, the time taken to complete each sieving operation, the rate of sieving and the overall efficiency of the machine were noted, calculated, and recorded accordingly. This procedure was conducted for three separate times with respect to each weight and the average result taken. At the end of operation, the following performance criteria were determined.

- (a) The Machine Throughput Capacity was calculated using the formula:



27th October 2021

Available online at <https://conference.rsujnet.org/>

$$T_C = \frac{M_T}{t_T} \quad (16)$$

Where.

T_C = Throughput capacity (124Kg/hr)

M_T = Total mass of fines sieved (45.32Kg)

t_T = Total time to complete the sifting (1316sec)

(b) Sifting Capacity: This is the rate at which the machine sieves in kilogram per hour (kg/hr)

This was determined using the relation:

$$SC = \frac{M}{t} \quad (17)$$

Where.

SC = Sifting capacity (164kg/hr)

M = Mass of cassava mash loaded into the sieve (60kg)

t = Time taken to complete the sifting (1316secs)

(c) Machine Sifting Efficiency (SE): this is the percentage mass of time cassava mash separated after sifting.

This is calculated as.

$$SE = \frac{M-C}{M} \times 100\% \quad (18)$$

Where. M = Mass of cassava mash loaded into the sieve (60kg)

C = Sieved residue (14.68kg)

SE = 75.53%

3.4.1 Performance Evaluation Results

The performance evaluation results of the machine are presented in Table 1.

Table 1: Performance Test Results of the Garri Sifting Machine

S/N	(M_m) Mass of Mash entering Hopper (kg)	(M_f) Mass of Fines Collected (kg)	Mass of Chaff Collected (kg)	Time of Operation (sec)	Efficiency (%)	Sieving Rate (kg/s)
1	2.0	1.61	0.39	46	81	0.04
2	7.0	5.49	1.51	153	78	3
3	12.0	9.12	2.88	263	76	0.04
4	17.0	12.75	4.25	351	75	6
5	22.0	16.35	5.65	445	74	0.04
						7
						0.04
						8
						0.04
						9
	12	9.064	2.936	251.6		
	A					
	v					

The results reveal that the rate of sieving which relates directly to the efficiency of the machine is a function of the mass of dewatered cassava mash entering into the hopper. This was obvious from the fact that the efficiency reduced from 81% to 74%, relative to the mass of garri mash entering the hopper from 2 kg to 22 kg respectively.

The average results obtained revealed that 12 kg of dewatered grated cassava sieved had waste residue of 2.936 kg indicating 9.064 kg of the sample fully sieved in 251.6 seconds leading to sieving rate of 0.047 kg/s of the machine. The overall efficiency of the machine is approximately 76% which is an indication of the proper working of the garri sifting machine as compared to the existing design of a continuous flow type rotary garri sifting machine of 56% efficiency.

3.4.2 Physical Properties of Garri Mash

The physical properties considered in this were particle size density, bulk (pack and loose), angle of repose and moisture content.



27th October 2021

Available online at <https://conference.rsunet.org>

Table 2: Physical Parameters of Garri Mash

Parameter	Results
Moisture Content (%)	48.00
Particle Density (Kg/m ³)	1095.00
Pack Bulk Density (Kg/m ³)	682.00
Lose Bulk Density (Kg/m ³)	392.00
Angle of Repose (°)	40.00

3.4.3 Graphical Interpretation of Results

The results of the performance test were further interpreted graphically using Figures 2 and 3, as shown.

The Figure shows the relationship between the amount of sievate (fines) and the taken to collect them at the completion of the sieving operation.

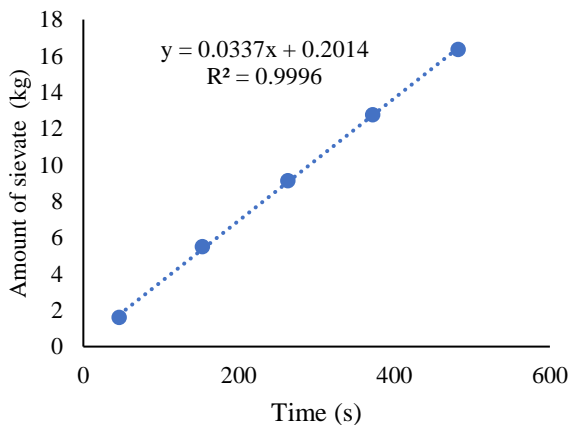


Figure 2: Relationship between the amount of fines collected and time of sieving

Table 3: Design Parameter

S/NO	PARAMETER	RESULTS
1	Design of Hopper	
	i. Volumetric Capacity	0.010752m ³
	ii. Total Surface Area	0.0489 m ³
2	Velocity of Belt	4.694m/s
3	Velocity Ratio of Belt Drive	0.42
4	Belt Length	0.8737m (874mm)
5	Power transmitted by the Belt	942.7W (0.94kw)
6	Belt Contact or Lap Angle θ_1	2.95 rad
	i. Belt Contact or Lap Angle θ_2	3.32 rad
7	Design of Pulley	
	i. Diameter of Driver Pulley	52mm
	ii. Diameter of Driven Pulley	108mm
8	Design of Shaft	
	i. Determination of shaft diameter	15mm
	ii. Bending Stress of the Shaft	108N/mm ²
	iii. Torsional Stress of the Shaft	7.4N/mm ²
9	Shear Forces and Bending Moment Diagrams	
10	Power Required to Rotate Pulverizing Shaft and Pulley	72.74W (0.1hp)
11	Design of Shaft Bearings	

From Figure 2, the curve establishes a linear relationship between the two variables, with a coefficient of determination (R^2) of 0.9996. The slope of the curve at any of the points will be a description of the rate of sieving during the operation.

Figure 3 is the curve of the relationship between the sieving efficiency and time taken to achieve the determined level of efficiency.

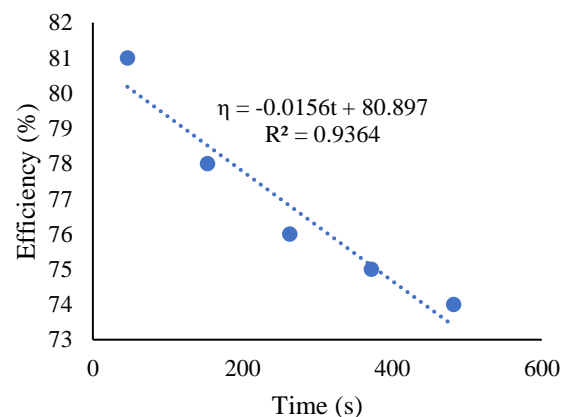


Figure 3: Relationship between sieving efficiency and time

The Figure 3 shows the relationship between efficiency and operational time for the sieving, characterized by the equation $\eta = - 0.015t +$



27th October 2021

Available online at <https://conference.rsujnet.org/>

80.897. The negative time coefficient and a coefficient of determination of 0.9364 are indicative of a decreasing machine efficiency with increasing time of operation. So, the machine performs better when the materials are loaded at an optimal rate. The results of the performance evaluation of the machine showed a throughput capacity of 124 kg/hr while the sifting capacity was 164 kg/hr with an average sifting rate of 0.047 kg/s, resulting in an overall sifting efficiency of approximately 76%. This is an indication that the efficiency compares favorably with other garri mash sifters designed and fabricated by authors such as Orojinmi (1997), Kudabo *et al.* (2012), Stephen *et al.* (2015), Ovat and Odey (2018). The development of this machine has improved the timeliness of the garri sifting process and eliminated the drudgery and hazards associated with the prevalent manual sifting process.

4.0 CONCLUSION

The development of an improved sifting machine for dewatered cassava mash was in response to the need to eliminate the drudgery and hazards of the current manual method in Nigeria. This machine has mechanized the process and enhanced the efficiency of operation up to about 76%. The machine can effectively and efficiently sift cassava mash of moisture content of 48%, which is in tandem with the findings of Kolawole *et al.* (2014). The angle of repose of 40° also corroborates the work of Lumay *et al.* (2012). A throughput capacity of 124 kg/hr, sifting capacity of 164 kg/hr and an overall machine efficiency of 76%, implies that the machine will contribute tremendously to enhancing the quality of life of the people.

REFERENCES

Ahiakwo, A. A., Isirima, C.B., & Inimgba, D.G. (2015). Appraisal and Projection of Cassava Mash Sieving Technology. *Net Journal of Agricultural Science*. 3(2): 49-55, ISSN: 2315-9766.

- Alabi, O. (2009). Design, Fabrication and Performance Evaluation of a Cassava Lump Breaking and Sieving Machine. An Unpublished HND Project. Department of Agricultural and Water Resources, Kwara State Polytechnic Ilorin, Kwara State.
- Alonge, A. F., Ekanem, S. S., & Ituen, U. U. (2012). Development of a Cassava Pelleting Machine. *Journal of Agricultural Engineering and Technology (JAET)*, 20(2): 29-37.
- Food and Agriculture Organization (1997). *Feeding Pigs in the Tropics*. Food and Agriculture Organization Animal Production and Health Paper 132. Rome
- Food and Agriculture Organization (1997). *Human Nutrition in the Developing World*. Food and Nutrition Series No. 29. Rome.
- Food and Agriculture Organization (2013). *A Textbook on Save and Grow Cassava: A guide to Sustainable Production Intensification*. Food and Agriculture Organization of the United Nation, Rome. 1-3.
- Food and Agriculture Organization (2013). *Agriculture Statistics for Food and Agriculture Organization*. European Union: Food and Agriculture Organization.
- Gupta, J. K., & Khurmi, R. S. (2005). *A Textbook on Machine Design*, 14th Edition, S. Chand Co. Ltd., New Delhi, 726-758.
- Hall, A. S., Holowenko, A. E., & Laughlin, H. G. (2002). *Schaum's Outline Series Theory and Problems of Machine Design*. (1st ed.). New York: McGraw-Hill Companies, Inc.
- Hassan, A. B., Matthew, S. A., Olugboji, O. A., & Ugwuoke, I. C. (2009). The Design and Construction of Maize Threshing Machine. *AU Journal of Technology*, 12(3): 199-206.
- Igoni, A. H. (1991). Design and Construction of a Continuous Flow Rotary-Type Sieving Machine for Gari Processing. *An Unpublished M.Sc. Thesis. Agricultural Engineering Department, University of Ibadan, Nigeria*. 101
- Kolawole, P., Abass, A., Agbetoye, L., Ogunlowo, S., & Odigbo, E. (2014). Some



**PROCEEDINGS OF THE INTERNATIONAL CONFERENCE
ON NEW VIEWS IN ENGINEERING AND TECHNOLOGY
(ICNET) MAIDEN EDITION, FACULTY OF ENGINEERING,
RIVERS STATE UNIVERSITY, PORT HARCOURT, NIGERIA.**



27th October 2021

Available online at <https://conference.rsujnet.org/>

Flow

Properties of Cassava Mash in Handling.
*Journal of Experimental Agriculture
International*. 4(11): 1348-1354.

Kudabo, E. A., Onipede, E. A., & Adegbenro, A. A. (2012). Design, Fabrication and Performance Evaluation of an Improved Cassava Mash Sifter. *Journal of Agriculture and Veterinary Sciences*. 4:53-64.

Lumay, G., Boschini, F., Traina K., Bontempi, S., Cloots, R., & Vandewalle, N. (2012). *Measuring the Flow Properties of Powders and Grain*. Power Technology 224: 19-27. doi: 10.1016/j.powtec.2012.02.015.

Ndirika, V. I., & Onwualu, A. P. (2016). *Design Principles for Post-Harvest Machines*, First Edition, Naphtali Prints, Shomulu, Lagos, Nigeria. 108-121.

Orojinmi, M. A. (1997). Development of Cassava Siever. Unpublished HND project, Agricultural Engineering Department, Kwara State Polytechnic, Ilorin.

Ovat, F. A., & Odey S. O. (2018). Development and Performance Evaluation of a Motorized Garri Sieving Machine. *European Journal of Advances in Engineering and Technology*. 5(7): 459-465.

Stephen, T., Dan-orawari, G.I., Aziaka, D.S., Ayejah, V. (2015). Design Analysis of a Reciprocating Cassava Sieving Machine. *IOSR Journal of Mechanical and Civil Engineering (IOSR-JMCE)*. 4(12): 07-15.

Sulaiman, M. A., & Adigun, R. A. (2005). Fabrication of Cassava Lump Breaker. *An Unpublished Project Report Submitted to the Department of Mechanical Engineering, Kwara State Polytechnic, Ilorin*

27th October 2021

Available online at <https://conference.rsujnet.org/>

APPENDIX

Isometric and Orthographic Drawings of the Garri Sifting Machine

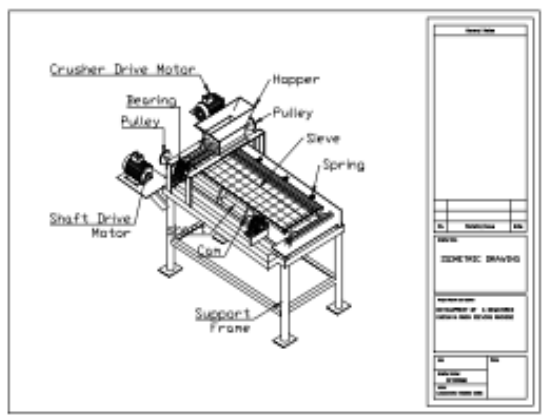


Fig 4: Isometric Drawing

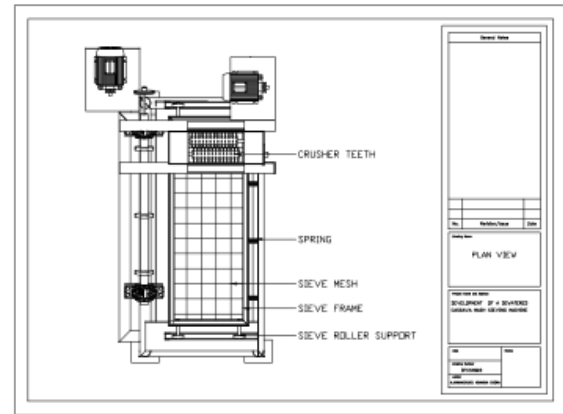
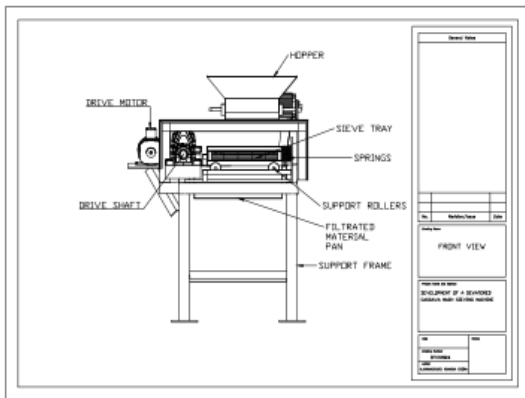


Fig 5: Plan View of Garri Sifting Machine



View

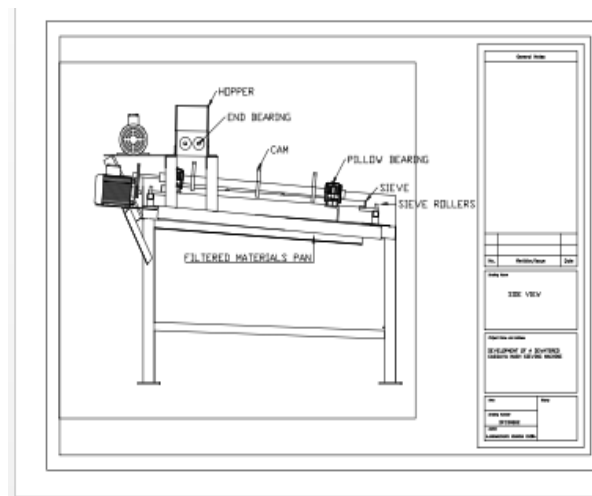


Fig7: Side View

Fig 6: Front